u = flow rate per unit area, $[Lt^{-1}]$
v = front velocity, $[Lt^{-1}]$
w = parameter defined by Eq. 10b, dimensionless
x = space coordinate, $[L]$
y = space coordinate, $[L]$
z = space coordinate, $[L]$
z_1 = parameter defined by Eq. 7, dimensionless

Greek Letters

α = wave number, $[L^{-1}]$
γ = density ratio, dimensionless
δ = amplitude of front displacement, dimensionless
ϵ = porosity, dimensionless
ζ = normalized temperature gradient, dimensionless
θ = perturbation in temperature, dimensionless
Λ = heat transfer parameter, dimensionless
μ = viscosity, $[ML^{-1}t^{-1}]$
ξ = space coordinate, $[L]$
ρ = density, $[ML^{-3}]$
σ = normalized perturbation length, dimensionless
ν = perturbation in velocity, dimensionless
ϕ = perturbation in velocity potential, dimensionless

Subscripts

D = dimensionless
f = surrounding formations
i = initial
R = reservoir
s = steam
w = water

Superscripts

o = referring to zero heat losses
$\sim$ = referring to perturbed quantities

LITERATURE CITED

Armento, M. E., and L. A. Miller, "Stability of Moving Combustion Fronts in Porous Media," *Soc. Pet. Eng. J.*, **17**, 423 (1977).

Baker, P. E., "Effect of Pressure and Rate on Steam Zone Development in Steamflooding," *Soc. Pet. Eng. J.*, **13**, 274 (1973).

Bear, J., *Dynamics of Fluids in Porous Media*, Elsevier, New York (1972).

Miller, C. A., "Stability of Moving Surfaces in Fluid Systems with Heat and Mass Transport. II: Combined Effects of Transport and Density Difference Between Phases," *AIChE J.*, **19**, 909 (1973).

———, "Stability of Moving Surfaces in Fluid Systems with Heat and Mass Transport. III: Stability of Displacement Fronts in Porous Media," *AIChE J.*, **21**, 474 (1975).

Saffman, P. G., and G. I. Taylor, "The Penetration of a Fluid into a Porous Medium or Hele-Shaw Cell Containing a More Viscous Liquid," Proc. Roy. Soc. (London), **A245**, 312 (1958).

Yortsos, Y. C., and G. R. Gavalas, "Heat Transfer Ahead of Moving Condensation Fronts in Thermal Oil Recovery Processes" *Int. J. Heat Mass Transfer*, **25** 3, 305 (1982).

———, "Analytical Modeling of Oil Recovery by Steam Injection. Part 2: Asymptotic and Approximate Solutions," *Soc. Pet. Eng. J.*, **21**, 179 (1981).

Manuscript received December 8, 1980; revision received June 23, and accepted July 14, 1981.

Finite Difference Calculation of Current Distributions at Polarized Electrodes

The changing geometry of electrodes undergoing electrodeposition or dissolution can be simulated by successive solutions of Laplace's equation with nonlinear boundary conditions. To overcome the instability in the finite-difference calculation caused by nonlinear boundary conditions, a weighting algorithm to compute the new surface potential on successive iterations has been developed.

G. A. PRENTICE
and
C. W. TOBIAS

Lawrence Berkeley Laboratory and Department of Chemical Engineering, University of California, Berkeley, CA 94720

SCOPE

In electrochemical reactors distribution of reaction rates on the electrode surfaces depends on cell geometry, electrolyte conductivity, charge transfer reaction kinetics, and on the rates of transport of reactants and products to and from reaction sites. The local reaction rate is proportional to the normal flux (current density) at that point. Determination of the potential field in the cell yields the distribution of the electric flux, and hence the distribution of reaction rates.

Except for the simplest of geometries and of kinetic, and mass-transfer conditions, problems of current distribution may be solved only through numerical techniques. This is particularly evident if one considers systems in which the electrode geometry changes as a result of the progress of the surface reaction.

The calculation of local reaction rates at electrode surfaces is generally the crucial step in modeling electrochemical systems. This implies that one must first compute potential and concentration distributions from which the local current densities can be obtained. In general, this problem requires the solution of multi-dimensional partial differential equations with nonlinear boundary conditions, which cannot be solved by elementary analytical techniques, unless simplifying assumptions are invoked. For example, if the electrodes are assumed to be at fixed potentials, and the cell is of a standard symmetric design, the current distribution can be obtained directly from a solution of the classical Dirichlet problem.

The first systematic study of current distribution problems

G. A. Prentice is presently at the Department of Chemical Engineering, The Johns Hopkins University, Baltimore, MD 21218.

ISSN-0001-1541-82-4282-0486-$2.00.

was presented by Kasper in a series of papers in the early 1940's. He recognized the mathematical equivalence of electrochemical problems and the classical problems of mathematical physics in fields such as electrostatics and gravitation. Analytical techniques such as direct integration, the method of images, and conformal mapping were applied to well-defined cell shapes (concentric cylinders, line-plane geometries, etc.) to solve for the current density distribution.

In any practical electrochemical system the electrode surface potential, measured with a reference electrode of the same kind as the working electrode, is differnt from that of the electrode. This difference, designated the overpotential, cannot be neglected in most systems. In general, the local overpotential increases with an increase in local current density.

Electrochemical problems are conveniently classified according to the rate limiting factor: the primary current distribution for ohmically limited systems, the secondary current distribution for kinetically controlled systems, and the tertiary current distribution for mass transport limited systems. The primary current distribution can be obtained from a solution of the Dirichlet problem; Neumann boundary conditions apply on insulated surfaces. For the simplest secondary current distribution problem, the overpotential is assumed to vary linearly with current density, and the problem becomes that of solving Laplace's equation with boundary conditions of the third kind. The general secondary and tertiary current distribution problems require the solution of Laplace's equation with nonlinear boundary conditions. Newman (1966) first calculated the tertiary current distribution on a rotating disk electrode, and later, together with Parrish (1969), computed the tertiary current distribution for a flow channel with plane parallel electrodes embedded in insulating walls.

In the literature the preponderance of current distribution problems solved by analytical techniques involves the primary current distribution. As high speed computers became widely available in the 1960's, more powerful numerical methods were applied to current distribution problems. Klingert et al. (1964) outlined a procedure for computing primary and secondary current distributions by the finite-difference method. Techniques for improving the computational efficiency of the finite difference method were presented by Fleck et al. (1964). This report also lists the current distribution problems that had been solved by analytical techniques.

For systems with inert electrodes, the current density distribution is time-invariant. Electrolyzers and redox cells are examples of systems with relatively inert electrodes. In other industrially significant processes such as aluminum reduction and electrochemical machining, the electrodes change shape, and the current distribution varies with time. Because of the necessity to recompute the current distribution on the changing electrode profile, analytical solutions are extremely rare. Wagner (1954) was the first to solve a non-trivial electrochemical moving boundary problem by analytical techniques. For a diffusion-controlled anodic process he derived an expression for the time-dependent change in apparent amplitude of a sinusoidal electrode. Subsequently, more complicated problems were solved by numerical techniques. Riggs et al. (1981) used the finite-difference method to model an electrochemical machining process. Prior work on modeling electrochemical machining is listed in Riggs et al. The finite element method was employed by Alkire et al. (1978) to investigate the shape change of a cathode in a rectangular cell.

Although there is an extensive literature on solving the Dirichlet problem, far fewer references regarding the solutions of Laplace's equation with nonlinear boundary conditions are available. A review of numerical solutions and techniques for current distribution problems has been presented by Prentice and Tobias (1982a). The goal of our work is to develop general techniques to solve time-dependent electrochemical problems by the finite-difference method. Since analogous equations arise in other problems involving transport phenomena, the methods presented should be applicable to those problems as well.

CONCLUSIONS AND SIGNIFICANCE

We have developed a general algorithm for use in conjunction with the finite-difference method for solving Laplace's equation with nonlinear boundary conditions. In this algorithm the surface potential is weighted with respect to four variables which indicate the tendency of the system toward numerical instability. Recomputation of the weighting factor when the surface potential is re-evaluated was shown to be computationally more efficient than the optimal constant weighting factor in the problem considered. Application of this algorithm to electrochemical cells yields potential and current distributions where both ohmic and kinetic effects are important. For systems where the diffusion layer on an electrode can be estimated, mass transport effects can be incorporated.

The time-dependent behavior of an electrode can be simulated through application of these methods to successively generated electrode profiles. The simulation of changing electrode contours is of interest in applications such as plating, electrochemical machining, and electroforming. In the present work we have illustrated the effects of variations in kinetic and mass transport parameters on the transient behavior of an initially sinusoidal electrode. Elsewhere we have simulated other cell arrangements (Prentice and Tobias 1982b) and have demonstrated good agreement with experimentally obtained transient electrode contours (Prentice and Tobias 1982c). In addition, the methods presented should be applicable to other systems where analogous equations arise.

EQUATIONS

In a well-stirred electrochemical system no concentration gradients are present in the bulk electrolyte, and the potential obeys Laplace's equation

$$\nabla^2\phi = 0 \tag{1}$$

At the electrode surface the normal current density is proportional to the local potential gradient

$$i_n = -\kappa\nabla_n^{\phi} \tag{2}$$

The Butler-Volmer equation describes the system kinetics for an electrode where the exchange current density i_o is insensitive to the reactant concentration

$$i_n = i_o\left[\exp\left(\frac{\alpha_a \mathrm{F}}{RT}\eta_s\right) - \exp\left(-\frac{\alpha_c \mathrm{F}}{RT}\eta_s\right)\right] \tag{3}$$

This expression relates the surface overpotential η_s to the normal current density i_n; the exchange current density i_o and the transfer coefficients α_a and α_c can be obtained from experimental data. A concentration gradient of the reacting species in a thin layer near an electrode causes an overpotential. If the concentration variation of the reacting species does not significantly change the electrolyte conductivity, the concentration overpotential can be approximated by

$$\eta_{cn} = \frac{RT}{n\mathrm{F}}\ell n\,(1 - i/i_\ell) \tag{4}$$

where i_ℓ, the limiting current density, is the maximum (diffusion-limited) current density at which a given electrode reaction can proceed. At a higher current density some other electrode reaction will also occur. The total overpotential, which is comprised of surface overpotential and concentration overpotential, is defined by

$$\eta = V - \phi_o \tag{5}$$

V is the electrode potential and ϕ_o is the potential adjacent to the electrode surface. Equations 2 and 5 serve as the general boundary conditions for Laplace's equation. The overpotential in Eq. 5 is obtained from Eqs. 3 and 4, which are nonlinear. For the primary current distribution the overpotential in Eq. 5 is zero and $\phi_o = V$. The above equations are discussed in detail by Newman (1973). The current is determined by integrating the normal current density over the electrode surface.

$$I = \int_s i_n dA \tag{6}$$

If we specify an amount of charge to be passed, then the time increment in which this electrode process occurs is:

$$\Delta t = Q/I \tag{7}$$

The boundary of the electrode surface progresses in proportion to the normal current density at each point:

$$\Delta H = \frac{M}{zF\rho} i_n \, \Delta t \tag{8}$$

A dimensionless number useful in characterizing the secondary current distribution is the Wagner number

$$W = \frac{\kappa\left(\frac{\partial \eta_s}{\partial i}\right)_{i_{av}}}{L} \tag{9}$$

where L is a characteristic dimension of the system. For the primary current distribution the Wagner number of zero. As W increases a more uniform current distribution is obtained. An explicit expression for the partial derivative in Eq. 9 in terms of the current density cannot be obtained from Eq. 3, except in the special case of $\alpha_a = \alpha_c$. When the current density is either much smaller or much larger than the exchange current density, simpler forms of Eq. 3 can be obtained. At low current densities the exponentials can be expanded in a Maclaurin series, and the linear overpotential relation is obtained

$$\eta_s = \frac{RT}{i_0(\alpha_c + \alpha_a)F} i \tag{10}$$

At high values of overpotential, one of the exponential terms of Eq. 3 becomes negligible. If we consider a large overpotential at the cathode, we obtain the Tafel relation

$$\eta_s = \frac{RT}{\alpha_c F} \ell n \, (|i|/i_o) \tag{11}$$

An advantage of using one of these forms is that the surface overpotential appears explicitly, and an analytical expression can always be obtained for the partial derivatives in Eq. 9.

NUMERICAL METHODS

Basic Procedure

In order to illustrate some of the features of the computational procedure, we chose to examine the behavior of a sinusoidal profile undergoing deposition. The grid network is shown in Figure 1. For problems considered in the present work, the anode is assumed to be at a fixed potential. For convenience, we restricted this study to cases where the Tafel form (Eq. 11) is valid. With these restrictions different cases can more easily be compared. Incorporation of the Butler-Volmer equation causes no special computational difficulties; its use in simulations of experimental systems is illustrated in Prentice (1981).

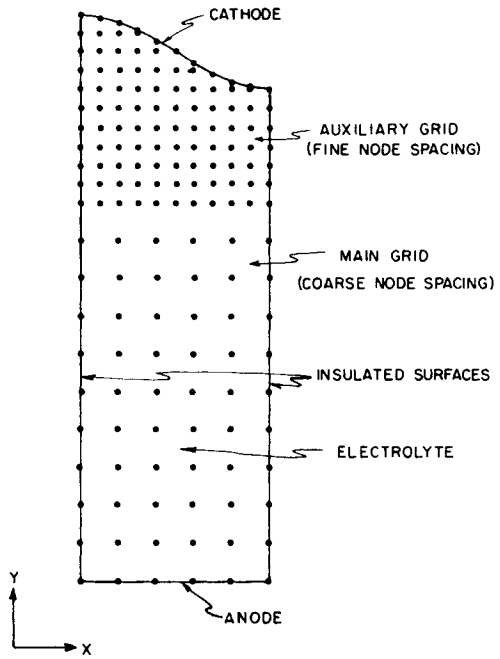

Figure 1. Schematic of the grid for the sinusoidal cathode problem.

The basic procedure to calculate successive profiles is as follows:

1. Specify boundary coordinates, physical properties, polarization parameters (α and i_o), grid spacing, convergence criteria, and time step size.
2. Estimate the initial potential distribution.
3. Construct piecewise polynomials through the boundary points so that derivatives at the surface can be calculated.
4. Obtain a loosely converged estimate of the solution to Laplace's equation. Tighten the convergence criterion as the iteration proceeds.
5. Calculate the normal current density by numerically differentiating the potential at each surface node.
6. Determine the overpotential from the polarization equation.
7. Calculate the surface potential from Eq. 5; weight this value with the value obtained from the previous iteration. If the potentials and currents meet the convergence criteria, proceed to step 8; otherwise, continue iteration at step 4.
8. Move each surface node normal to the surface in proportion to the charge passed.
9. Construct interpolating polynomials to determine the new ordinates at evenly spaced abscissa points.

For the primary current distribution Laplace's equation need only be solved once, and step 7 is eliminated. A detailed description of the numerical procedure is presented by Prentice (1981).

Computational Techniques

The finite-difference method, coupled with successful overrelaxation, is used to calculate the potential distribution in the bulk. Fleck's (1964) results indicated that an overrelaxation parameter of 1.8 to 2.0 gave the greatest computational efficiency. We use 1.85 in all of our simulations. A method outlined in Lapidus (1962) is used to approximate the potential at nodes adjacent to the surface.

A three point numerical differentiation formula is used to calculate the current density at each surface node. The electric field normal to the surface is calculated from the projections of the X and Y components on the normal. The current density at the surface is the product of the conductivity and the field. This approximation for the current density is substituted into Eq. 4 and 11 to get an estimate of the overpotential. The surface potential is then

obtained from Eq. 5. Before using this estimate for the surface potential in the next iteration, it is weighted with the surface potential from the previous iteration.

$$\phi_o^{(r+1)} = \phi_o^{(r-1)} + D(\phi_o^{(r)} - \phi_o^{(r-1)}) \qquad (12)$$

where D is a weighting factor which varies between 0 and 1. The surface potentials are checked for convergence before the weighting procedure is performed. When the surface potentials meet the convergence criterion, the weighting factor is reduced on successive iterations until the normalized change in current density between iterations also meets the specified error criterion.

When convergence is attained, the boundary is moved in proportion to the normal current density in Eq. 8. The interpolating polynomials of the cubic spline, described in Ahlberg et al. (1967), are used to interpolate back to the original abscissa coordinates. If the profiles tend toward discontinuous behavior, least squares smoothing can be performed before interpolating.

Convergence Procedure

In order to obtain a converged solution, a judicious choice of the factor D in Eq. 12 must be made. A value of D equal to one implies direct substitution. For small values of W (less than 0.1), a value of D equal to one will frequently lead to a converged solution; however, for larger values of W, the oscillatory behavior of the surface potentials may lead to instabilities. Intuitively, one might expect that a converged solution could always be obtained if one were to choose a sufficiently small value of D. One would like to choose a value of D that is small enough to avoid oscillatory instabilities, yet large enough to avoid an excessive number of iterations. Such an optimum choice is difficult to make *a priori*.

Rather than choosing a constant value for D, we have devised an algorithm from which a value for D is calculated each time the surface potential is re-evaluated. In this programmed weighting algorithm, the value of D is dependent on four variables: (1) the consistency of the direction of change of the surface potential at a specified point; (2) the normalized change in current density between iterations; (3) the normalized change in surface potentials between iterations; and (4) the Wagner number.

The evaluation of the current density requires a numerical differentiation of the potentials at the electrode surface (Eq. 2). Since this numerical differentiation is sensitive to small changes in adjacent bulk electrolyte potentials, we specified that a somewhat restrictive (10^{-4}), though larger than the final (10^{-6}), convergence criterion, defined by $(\phi^{(r)} - \phi^{(r-1)})/\phi^{(r)}$, be attained before evaluating the current densities. As a converged solution is approached, and the relative change in surface potentials decreases, the convergence criterion that must be attained before evaluating the current densities decreases. The overpotentials and surface potentials are determined from Eqs. 4, 5, and 11. With the new values of the surface potentials, the relative change in these surface potentials from the previous iteration can be calculated. By calculating these changes prior to weighting, we obtain a measure of the convergence.

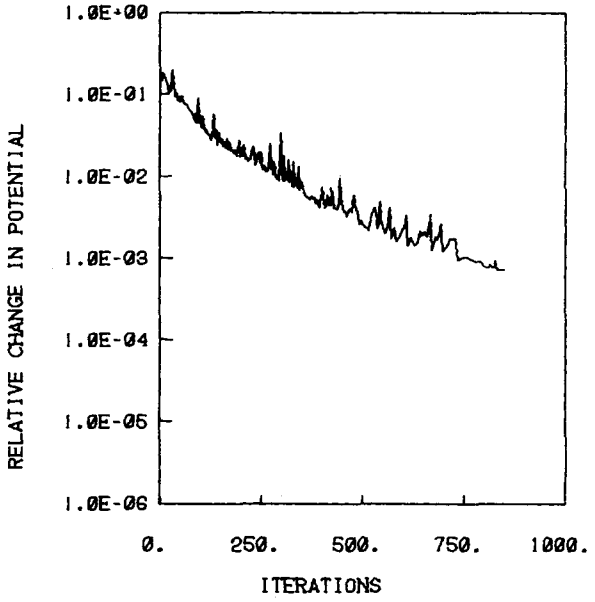

Figure 3. Normalized maximum change in surface potential. W = 25. Time step 1.

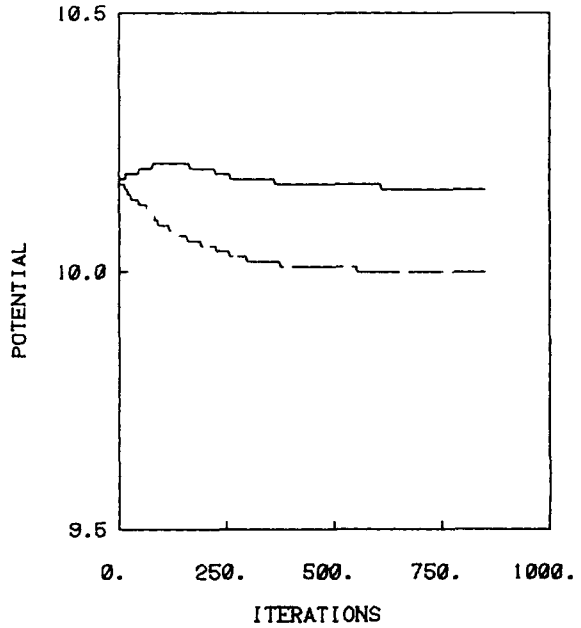

Figure 2. Surface potential at peak and in the depression (dashed). W = 25. Time step 1.

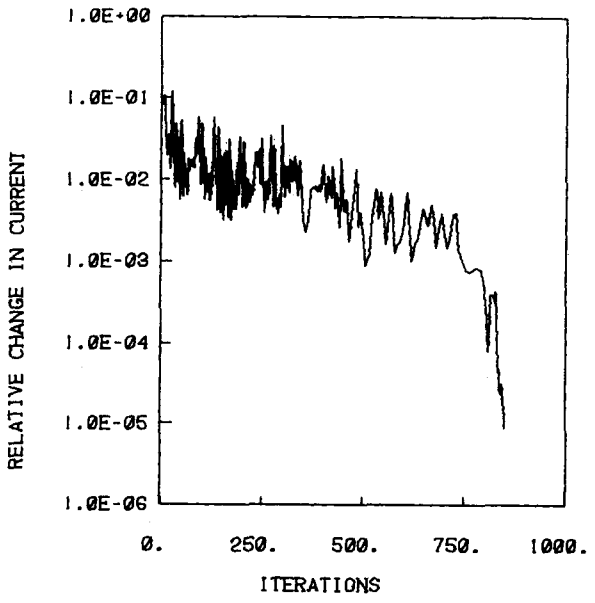

Figure 4. Normalized average change in current density. W = 25. Time step 1.

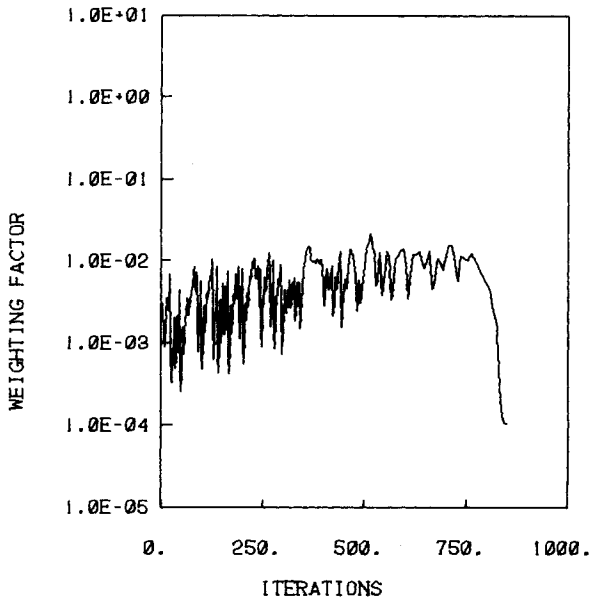

Figure 5. Weighting factor for surface potentials. W = 25. Time step 1.

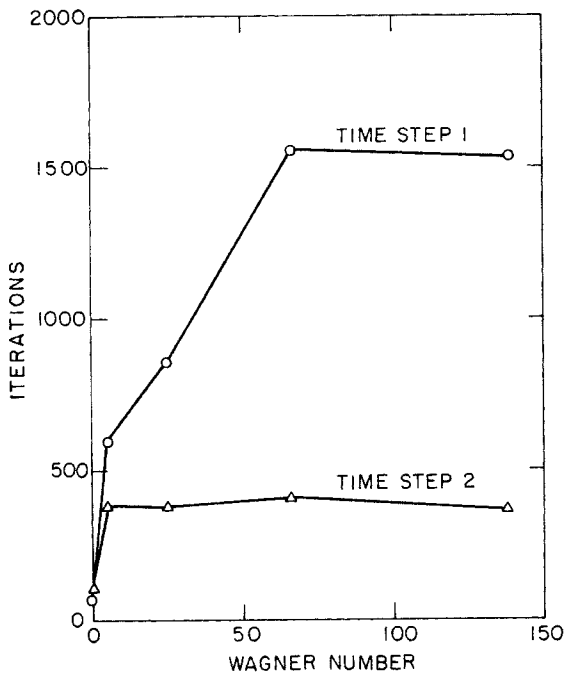

Figure 6. Number of iterations required for convergence of the first two time steps of the sinusoidal cathode simulations as a function of the Wagner number.

The four variables, noted above, are incorporated in functions to determine the weighting factor. If the surface potential at the specified node is proceeding in the same direction, this "consistency factor" is increased. If this surface potential begins to oscillate, the consistency factor is reduced; large oscillations indicate incipient instability. Small oscillations frequently indicate an approach to convergence. The "current factor" is increased if the average normalized change in current density is smaller than specified limits (on the order of a few percent); the current factor is reduced if the change is large. The limits are functions of the Wagner number and the consistency factor. The normalized change in surface potential indicates the degree of convergence. As this variable approaches the convergence criterion, the weighting factor is reduced. When the weighting factor is reduced sufficiently, the average current error also decreases until the error criterion for that variable is also met.

RESULTS

The behavior of the surface potentials, the maximum normalized change in surface potentials, the average normalized change in current density, and the weighting factor are illustrated in Figures 2, 3, 4, and 5, respectively, for the problem of deposition on a sinusoidal profile with W = 25 for the first time step. For these problems we selected convergence criteria for the bulk potentials, the current densities, and the surface potentials of 10^{-6}, 10^{-5}, and 10^{-3}, respectively. The surface potential at the profile peak (Figure 2) increases before reaching the final converged value. Without the weighting factor to attenuate this oscillatory behavior, convergence would not be attained.The curves are not smooth since the surface potentials are not re-evaluated each time the bulk potentials are recomputed. The weighting factor D (Figure 5) tends to increase as the current density variations (Figure 4) stabilize. When the relative surface potential variation (Figure 3) reaches the convergence criterion (10^{-3}), the weighting factor is decreased.

The algorithm is sufficiently general so that converged solutions are obtainable over a wide range of Wagner numbers for the secondary current density problem (Figure 6). In the first time step the relatively large number of iterations is attributable to poor initial estimates. This is because the initial estimates for the first time step are obtained from a simple algorithm, while those for the second (and succeeding) time steps are obtained from converged solutions at the previous time step.

The results of the programmed weighting algorithm are compared with the results of selecting a value for D *a priori* for W = 25 (Figure 7). This graph illustrates the difficulty of choosing the optimum value for D. A small value (10^{-3}) for D results in a rather efficient computation for the second time step, but the first time step requires five times as many iterations as the programmed weighting technique. A value of D greater than 2×10^{-3} causes

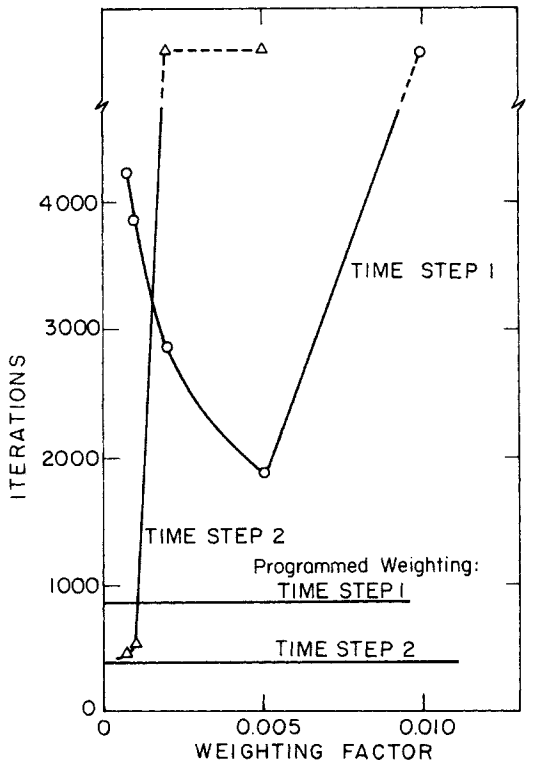

Figure 7. Comparison of the programmed weighting technique with a constant weighting factor method.

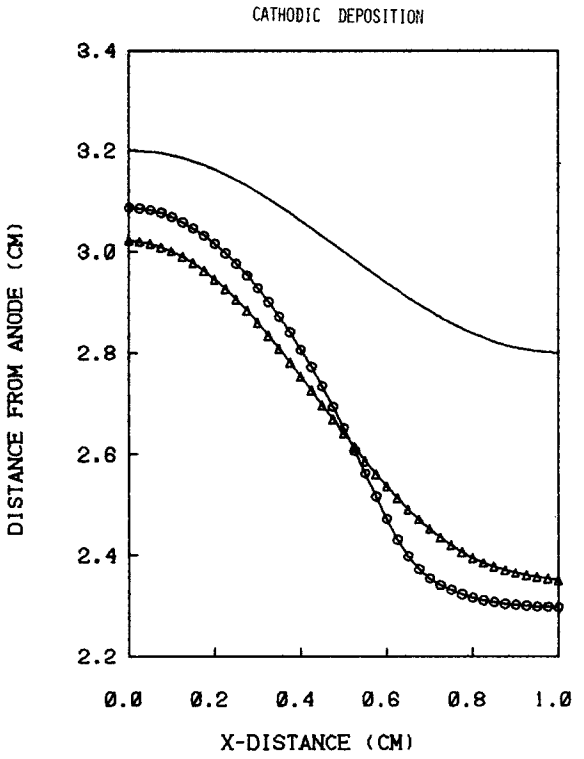

Figure 8. Half-wavelength of the sinusoidal moving boundary simulations. The upper curve is the original profile. The lower curves are the final profiles. Δ W = 1; o W = 0.5, 99% of the limiting current on the profile peak.

oscillations during the second time step, and convergence to the specified criteria does not occur. For this problem, converged solutions for the two-time steps were always obtained more quickly by using the programmed weighting algorithm than by using the optimum constant value for D of approximately 10^{-3}.

Results of time-dependent secondary and tertiary current distribution simulations are illustrated in Figure 8. In each case equal quantities of charge have been passed to obtain the final profiles. With the initial amplitudes taken as the characteristic length, the Wagner numbers for the two cases are approximately 0.5 and 1.0. In the former case mass transport effects were also considered. At the higher Wagner number kinetic resistance at the surface tends to even out the current distribution, and relatively uniform growth is achieved. For the tertiary current distribution the peak was held at 99% of the limiting current. A value of approximately 15 mV was used for RT/nF in Eq. 4. Since the overpotential increases rapidly at high fractions of the limiting current, the peak becomes flatter than for the secondary current distribution. In the tertiary distribution case, the current distribution is relatively nonuniform.

With the stringent convergence criteria for the problems considered in this study, execution time on the order of 10 s per time step on a CDC 7600 was required. Twelve-time steps were used to generate each profile in Figure 8.

Other cell arrangements have been studied using this weighting technique. Deposition on a corner electrode and in a notch shaped electrode have been presented by Prentice (1981).

ACKNOWLEDGMENT

This research was supported by the Division of Energy Storage Systems, Office of Conservation and Renewable Energy, U.S. Department of Energy, under Contract No. W-7405-ENG-48.

NOTATION

A = area (m^2)
D = weighting factor
F = Faraday, 96,500 C
H = distance (m)
i = current density (A/m^2)
i_o = exchange current density (A/m^2)
I = current (A)
M = atomic weight (g/mol)
n = number of electrons participating in an electrode reaction
Q = charge (C)
R = gas constant, 8.32 J/mol·K
S = surface
T = temperature (K)
t = time (s)
V = electrode potential (V)
W = Wagner number
X,Y = cartesian coordinates
z = equivalents/mol

Subscripts

a = anode
c = cathode
cn = concentration
ℓ = limiting
n = normal
s = surface

Superscripts

r = iteration number

Greek Symbols

α = transfer coefficient
η = overpotential (V)
κ = electrolyte conductivity ($ohm^{-1}m^{-1}$)
ϕ = potential (V)
ϕ_o = potential adjacent to an electrode surface (V)

LITERATURE CITED

Ahlberg, A. J., E. N. Nilson, and J. L. Walsh, "The Theory of Splines and Their Applications," Academic Press, New York (1967).

Alkire, R., T. Bergh, and R. L. Sani, "Predicting Electrode Shape Change with Use of Finite Element Methods," *J. Electrochem. Soc.*, **125**, 1981 (1978).

Fleck, R. N., D. N. Hanson, and C. W. Tobias, "Numerical Evaluation of Current Distribution in Electrochemical Systems," Lawrence Radiation Laboratory, Berkeley, CA (September, 1964) (UCRL-11612).

Kasper, C., "Theory of the Potential and Technical Practice of Electrodeposition," *Trans. Electrochem. Soc.*, **77**, 353 (1940); **77**, 365 (1940); **78**, 131 (1940); **78**, 147 (1940); **82**, 153 (1942).

Klingert, J. A., S. Lynn, and C. W. Tobias, "Evaluation of Current Distribution in Electrode Systems by High-Speed Digital Computers," *Electrochimica Acta*, **9**, 297 (1964).

Lapidus, L., "Digital Computation for Chemical Engineers," McGraw-Hill, New York (1962).

Newman, J., "Current Distribution on a Rotating Disk below the Limiting Current," *J. Electrochem. Soc.*, **113**, 1235 (1966).

Newman, J., "Electrochemical Systems," Prentice-Hall, Englewood Cliffs, NJ (1973).

Parrish, W. R., and J. Newman, "Current Distribution on a Plane Electrode below the Limiting Current," *J. Electrochem. Soc.*, **116**, 169 (1969).

Prentice, G. A., "Modeling of Changing Electrode Profiles," Ph.D. Thesis, Department of Chemical Engineering, University of California, Berkeley (1981), or Lawrence Berkeley Laboratory Report (December, 1980) (LBL-11694).

Prentice, G. A., and C. W. Tobias, "A Survey of Numerical Methods and Solutions for Current Distribution Problems," *J. Electrochem. Soc.*, **129**, 72 (1982a).
Prentice, G. A., and C. W. Tobias, "Simulation of Changing Electrode Profiles," *J. Electrochem. Soc.*, **129**, 78 (1982b).
Prentice, G. A. and C. W. Tobias, "Deposition and Dissolution on Sinusoidal Electrodes," *J. Electrochem. Soc.*, **129**, 316 (1982c).
Riggs, J. B., R. H. Muller and C. W. Tobias, "Prediction of Work Piece Geometry in Electrochemical Cavity Sinking," *Electrochimica Acta*, **26**, 961 (1981).
Wagner, C., "A Contribution to the Theory of Electropolishing," *J. Electrochem. Soc.*, **101**, 225 (1954).

Manuscript received January 12, 1981, revision received June 15, and accepted July 14, 1981.

Analysis of Batch, Dispersed-Emulsion, Separation Systems

An analysis of a batch, dispersed-emulsion (liquid membrane), separation system results in simple models that describe the concentrations and masses of each phase as functions of time. Comparisons with a limited set of experimental data are offered. One of these models allows a set of pilot studies to be extended to performance predictions and comparative studies of different feed-membrane-solvent combinations, which could lead to an optimally designed separation process.

V. J. KREMESEC, JR. and J. C. SLATTERY

Department of Chemical Engineering
Northwestern University
Evanston, IL 60201

SCOPE

A liquid membrane separation system is comprised of three liquid phases. Two miscible phases are separated from each other by a third membrane phase that is insoluble with both. The interfaces are stabilized by a surfactant. The rate of mass transfer between the two miscible phases is controlled by the rate of mass transfer across the liquid membrane phase. Such systems were introduced by Li (1971a and b), who separated hydrocarbons by taking advantage of the differences among their solubilities in an aqueous membrane.

In waste water treatment (Li and Shrier, 1972) and in the removal of toxic agents from blood streams (Asher et al., 1975), a compound is transferred from one aqueous phase, across an oil membrane, into another aqueous phase where it undergoes a chemical reaction. The product of the reaction cannot cross the oil membrane because of solubility limitations.

In facilitated transport systems, a carrier molecule is placed in the liquid membrane phase (Caracciolo et al., 1975). This carrier reacts selectively with an ionic species at an interface and diffuses to the opposite interface where it releases the ion. Such a system has been demonstrated in concentrating chromium against its concentration gradient (Hochhauser and Cussler, 1975).

Two configurations of liquid membrane systems have been considered for application.

In one configuration, a mesh or porous material is saturated with the membrane phase and is placed between the solvent and feed phases. This configuration has been studied extensively and analyses have been developed to the point where data correlations and comparative studies are possible (Caracciolo et al., 1975; Schultz et al., 1974; Lee et al., 1978).

A second configuration employs a dispersed emulsion in a stirred tank (Li, 1971b; Li and Shrier, 1972; Hochhauser and Cussler, 1975). The first step is to emulsify the feed and membrane phases. This emulsion is then dispersed in the continuous solvent phase. Although experimental results indicate that this scheme is feasible (Lee et al., 1978), an analysis has not been developed that is adequate for data correlations or comparative studies. Boyadzhiev et al. (1977) have recognized in their analysis that the volumes of the phases change with time, but they assumed that the mass densities of the phases are independent of time. This would not be justified generally even for the heptane-toluene-kerosene system they studied.

Our objective is to construct an analysis for a batch, dispersed-emulsion (liquid-membrane), separation system that is adequate for data correlations or comparative studies. The components of the feed separate, because their solubilities and diffusion coefficients in the membrane differ, resulting in different rates of mass transfer across the membrane. Interphase mass transfer is described in terms of mass transfer coefficients. The masses of the feed and of the solvent phases are allowed to vary with time. The concentrations of a species on either side of an interface are related by distribution coefficients. The use of this analysis is illustrated with a limited set of experimental data.

CONCLUSIONS AND SIGNIFICANCE

An approximate analysis of a batch, dispersed-emulsion (liquid-membrane), separation system results in two simple models that describe the concentrations and masses of each phase as functions of time. The simplified variable mass model allows the masses of the feed and solvent phases to vary with time; the simplified fixed mass model assumes that the masses of the phases are independent of time. Both of these simplified models assume that the initial concentrations and masses are known and that the distribution coefficients appearing in the models can be calculated independently as functions of the concentrations.

For an N component system, the simplified variable mass

V. J. Kremesec, Jr. is presently with Amoco Production Co., Tulsa, OK 74102.

ISSN-0001-1541-82-4182-0492-$2.00